

# VL-NMS: Breaking Proposal Bottlenecks in Two-Stage Visual-Language Matching

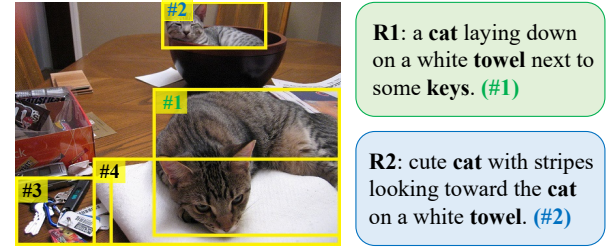
Wenbo Ma, Long Chen, Hanwang Zhang *Member IEEE*, Jian Shao *Member IEEE*,  
Yueting Zhuang *Member IEEE*, Jun Xiao *Member IEEE*

**Abstract**—The prevailing framework for matching multimodal inputs is based on a two-stage process: 1) detecting proposals with an object detector and 2) matching text queries with proposals. Existing two-stage solutions mostly focus on the matching step. In this paper, we argue that these methods overlook an obvious *mismatch* between the roles of proposals in the two stages: they generate proposals solely based on the detection confidence (*i.e.*, query-agnostic), hoping that the proposals contain all instances mentioned in the text query (*i.e.*, query-aware). Due to this mismatch, chances are that proposals relevant to the text query are suppressed during the filtering process, which in turn bounds the matching performance. To this end, we propose VL-NMS, which is the first method to yield query-aware proposals at the first stage. VL-NMS regards all mentioned instances as critical objects, and introduces a lightweight module to predict a score for aligning each proposal with a critical object. These scores can guide the NMS operation to filter out proposals irrelevant to the text query, increasing the recall of critical objects, resulting in a significantly improved matching performance. Since VL-NMS is agnostic to the matching step, it can be easily integrated into any state-of-the-art two-stage matching methods. We validate the effectiveness of VL-NMS on two multimodal matching tasks, namely referring expression grounding and image-text matching. Extensive ablation studies on several baselines and benchmarks consistently demonstrate the superiority of VL-NMS.

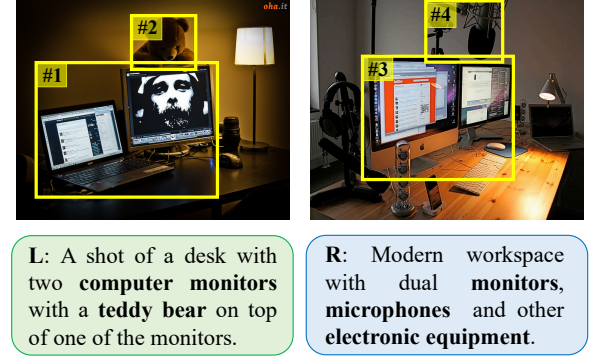
**Index Terms**—Text-guided Region Proposal Generation, Visual Grounding, Image-Text Matching, Non-Maximum Suppression

## I. INTRODUCTION

**R**ECENTLY, visual-language tasks which require jointly reasoning over both vision and natural language modalities have attracted great interest in the multimedia community. Matching multimodal inputs is one of the most fundamental abilities that can facilitate many high-level visual-language tasks. Considering different granularities of matching, there are two types of tasks: 1) **Instance-level matching**, where each text query refers to one targeted instance (referent) in the image and is explicitly grounded to one image region, *e.g.*, the Referring Expression Grounding (REG) task [1, 2, 3]. 2) **Image-level matching**, where text queries describe the whole image and are matched with images holistically, *e.g.*, the Image-Text Matching (ITM) task [4, 5, 6]. Both two types of tasks are important for many downstream applications such as



(a) An example of confusing referring expression.



(b) An example of confusing image-sentence pair.

Fig. 1. Confusing examples from REG and ITM tasks. (a): A referring expression comprehension example from RefCOCOg [11]. Two similar expressions (R1 and R2) refer to different objects. (b): An image-text matching example from MSCOCO [12]. Two similar images with overlapping visual content.

bidirectional cross-modal retrieval [7], visual question answering [8], visual navigation [9] and autonomous driving [10].

The vast majority of state-of-the-art visual-language matching methods are in a two-stage manner. At the first stage, a pretrained object detector is used to extract region proposals from images. At the second stage, these proposals are either treated as candidate bounding boxes (bboxes) to be selected from as in REG, or regressed as a bottom-up attention mechanism [13] as in ITM.

More specifically, two-stage REG methods normally divide the input query into components, ground each component to one proposal and reason about the interactions among them under the guidance of input query. Compared with one-stage grounding methods which regard REG as a generalized object detection (or segmentation) task, two-stage methods with the “detect-and-ground” pipeline is more similar to the human way of reasoning. More importantly, it’s much easier for two-stage methods to exploit the linguistic structure of referring expressions and perform global reasoning, which is vital when

W. Ma, J. Shao, Y. Zhuang and J. Xiao are with Zhejiang University, Hangzhou, 310027, China. Email: mwb@zju.edu.cn, jshao@cs.zju.edu.cn, yzhuang@zju.edu.cn, junx@zju.edu.cn.

L. Chen is with Columbia University, New York, 10027, USA. This work was partially done when L. Chen was a Ph.D. student at Zhejiang University. Email: zjuchenlong@gmail.com (Corresponding author).

H. Zhang is with Nanyang Technological University, Singapore, 639798. Email: hanwangzhang@ntu.edu.sg.

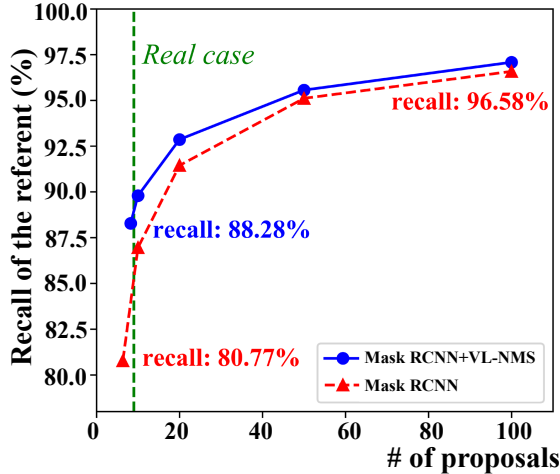


Fig. 2. The recall of the referent (IoU>0.5) vs. number of proposals on the RefCOCO testB set. The real case denotes the actual situation in all state-of-the-art two-stage grounding methods.

dealing with long, complex expressions. For example in Fig. 1 (a), when grounding “a cat laying down on a white towel next to some keys”, it is even difficult for humans to identify the referent *cat* without considering its contextual objects *towel* and *keys*. Also, it has been pointed out that one-stage methods are insensitive to linguistic variations. When changing the expression in Fig. 1 (a) to “cute cat with stripes looking toward the cat on a white towel”, they tend to refer to the same object (#1) [14]. In general, two-stage grounding methods with perfect proposals (e.g., all human-annotated object regions) can achieve more accurate and explainable grounding results than the one-stage counterparts.

On the other hand, two-stage ITM methods cross match region proposals with query words and use these local matching scores to measure the global image-sentence similarity. It has been widely recognized that by inferring the latent correspondence between each image region and each query word, two-stage ITM methods can better capture the fine grained interplay between vision and language and are more interpretable to human [4]. Take Fig. 1 (b) as an example. These two images contain overlapping visual content (monitors) which makes it difficult to distinguish them from one another on the image level. But by paying attention to other critical objects (e.g., teddy bear in the left image, microphones in the right image), two-stage methods have a better chance to match them with the right sentence.

However, the performance of two-stage visual-language matching methods is heavily bounded by the proposal quality. Especially for REG, when changing the proposals from human-annotated regions to detected regions of a pretrained detector, two-stage REG methods’ performance drops dramatically. In this paper, we argue that this huge performance gap between the detected and ground-truth proposals is mainly caused by the **mismatch** between the roles of proposals in the two stages: *the first-stage network generates proposals solely based on detection confidence, while the second-stage network just assumes that the generated proposals will contain*

**R: a person holding a slice of pizza.**

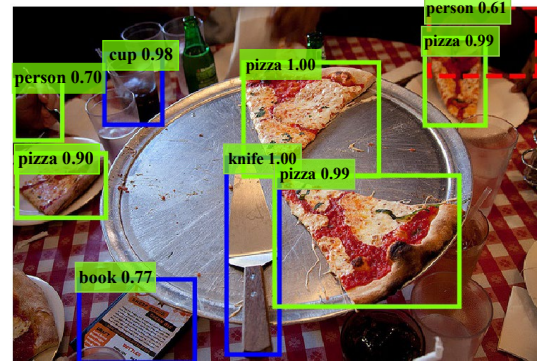


Fig. 3. An example of the first-stage proposals of prevailing MAttNet [1]. The proposals only contain bboxes with high detection confidence regardless of the content of expression (e.g., The candidates knife, book, and cup are not mentioned in expression). The bbox in red dashed line denotes the missing referent.

*all instances mentioned in the text query.* Take REG as an example. For each image, a well pre-trained detector can detect hundreds of detections with a near-perfect recall of the referent and contextual objects (e.g., as shown in Fig. 2, recall of the referent can reach up to 96.58% with top-100 detections). However, to relieve the burden of the referent grounding step in the second stage, current two-stage methods always filter proposals simply based on their detection confidences. These heuristic rules result in a sharp reduction of the recall (e.g., decrease to 80.77% as in Fig. 2), and bring in the mismatch negligently. To illustrate this further, we show a concrete example in Fig. 3. To ground the referent at the second stage, we hope that the proposals contain the referent *person* and its contextual object *pizza*. In contrast, the first-stage network only keeps bboxes with high detection confidence (e.g., knife, book, and cup) as proposals, but actually misses the critical referent *person* (i.e., the red bbox).

In this paper, we propose a novel algorithm VL-NMS, to rectify the mismatch of detected proposals at the conventional first stage. In particular, for each text query, VL-NMS regards all nouns in the text query as critical objects, and introduces a lightweight relatedness module to predict a probability score for each proposal to be a critical object. The higher predicted score denotes the higher relevance between a proposal and the text query. Then, we fuse the relatedness scores and classification scores, and adopt the fused scores as the suppression criterion in Non-Maximum Suppression (NMS). After NMS, we can filter out the proposals with little relevance to the text query. Finally, all proposals and the text query are fed into the second-stage grounding or matching network, to obtain the final prediction.

This paper is a substantial extension of our conference publication [15] with the following improvements. First, we propose an alternative way to build pseudo ground-truth by means of weakly supervised phrase grounding. Training VL-NMS no longer needs bbox annotations from COCO-detection dataset. Second, We extend VL-NMS to the image-text matching task. Extensive ablations demonstrate the superiority of

VL-NMS on this image-level matching task. Last, we demonstrate through experiments that VL-NMS is able to learn transferable fine grained correspondence between visual and language. This characteristic is extremely useful when bbox annotations are absent from the target tasks (*e.g.*, the image-text matching task). The contributions and novelty of this work are summarized as follows:

- We are the first to point out the proposal bottlenecks in two-stage visual-language matching methods. By investigating the recall of critical objects, we attribute the degraded performance of two-stage methods to the query-agnostic proposals generated at the first stage.
- We propose a novel algorithm VL-NMS to rectify the mismatch of proposals at the first stage by making the proposals query-aware. We also explore different ways to build pseudo ground-truth for training VL-NMS.
- We demonstrate significant performance gains on three REG benchmarks and one ITM benchmark. It's worth noting that VL-NMS can be generalized and easily integrated into any state-of-the-art two-stage grounding or matching methods to further boost their performance.
- Our method is efficient, generalizable and transferable, opening door for many downstream applications such as multimodal summarization.

## II. RELATED WORK

### A. Referring Expression Grounding

Considering different granularities of localization, there are two types of REG: 1) Referring Expression Comprehension (REC) [16, 17, 18, 19], where the referents are localized by bboxes. 2) Referring Expression Segmentation (RES) [20, 21, 22, 23], where the referents are localized by masks.

1) *Referring Expression Comprehension*: Current overwhelming majority of REC methods are in a two-stage manner: proposal generation and referent grounding. To the best of our knowledge, existing two-stage works all focus on the second stage. Specifically, they tend to design a more explainable reasoning process by structural modeling [1, 3, 2, 24, 25, 26], or more effective multi-modal interaction mechanism [27, 28]. However, their performance is strictly limited by the proposals from the first stage. Recently, another emerging direction to solve REC is in a one-stage manner [29, 30, 31, 32, 33]. Although one-stage methods achieve faster inference speed empirically, they come at a cost of lost interpretability and poor performance in composite expressions. In this paper, we rectify the overlooked mismatch in two-stage methods.

2) *Referring Expression Segmentation*: Unlike REC, most of RES works are one-stage methods. They typically utilize a “concatenation-convolution” design to combine the two different modalities: they first concatenate the expression feature with visual features at each location, and then use several conv-layers to fuse the multimodal features for mask generation. To further improve mask qualities, they usually enhance their backbones with more effective features by multi-scale feature fusion [23], feature progressive refinement [34, 35, 36], or novel attention mechanisms [22, 37, 38]. Besides, with the development of two-stage instance segmentation (*e.g.*, Mask

R-CNN [39]), two-stage REC methods can be extended to solve RES simply by applying the mask branch upon the predicted bounding box at the end of the second stage. Analogously, VL-NMS can be easily integrated into any two-stage RES method.

### B. Image-text Matching

Image-text matching aims to align images with sentences, normally evaluated by the recall of bidirectional retrieval. Prior works directly learn the global correspondence between images and sentences [40, 41, 42]. These works normally encode images and sentences into holistic feature vectors, project them into a common feature space and try to maximize the similarity between the matched image-sentence pairs. Recent works propose to infer the latent local correspondence between each image region and each word or noun chunk in the sentence [4, 5, 6]. By exploiting this fine grained correspondence, the global matching performance can be improved. This type of methods typically use a pretrained object detector to extract region proposals from images, then match them with each word in the sentence. VL-NMS can help to filter out region proposals irrelevant to the sentence and aid the local correspondence inference process.

### C. Phrase Grounding

Given an image and a sentence, phrase grounding aims to ground all noun phrases in the sentence. There are also two types of solutions: proposal-free methods and proposal-driven methods. Different from REC, the queries in phrase grounding are much simpler, which relieves two-stage methods from complicated relational reasoning and allows them to take more proposals at the second stage<sup>1</sup>. Meanwhile, efforts have been taken to handle the query diversity at the first stage by either using a object detector pre-trained on another large-scale dataset [43] or re-generate proposals with respect to queries and mentioned objects [44]. Recently, a large proportion of phrase grounding works turn to the weakly supervised setting where only image-sentence alignment is provided as annotation [45, 46, 47]. In this paper, we use weakly supervised phrase grounding as an alternative way to capture cross-modal context in generated region proposals.

### D. Non-Maximum Suppression

Non-Maximum Suppression (NMS) is a de facto standard post-processing step adopted by numerous modern object detectors, which removes duplicate bboxes based on detection confidence. Except for the most prevalent GreedyNMS, multiple improved variants have been proposed recently. Generally, they can be categorized into three groups: 1) Criterion-based [48, 49, 50, 51]: they utilize other scores instead of classification confidence as the criterion to remove bboxes by NMS, *e.g.*, IoU scores. 2) Learning-based [52, 53]: they directly learn an extra network to remove duplicate bboxes.

<sup>1</sup>At the second stage, REC methods take an average number of 10 proposals while phrase grounding methods can take more than 200 proposals.

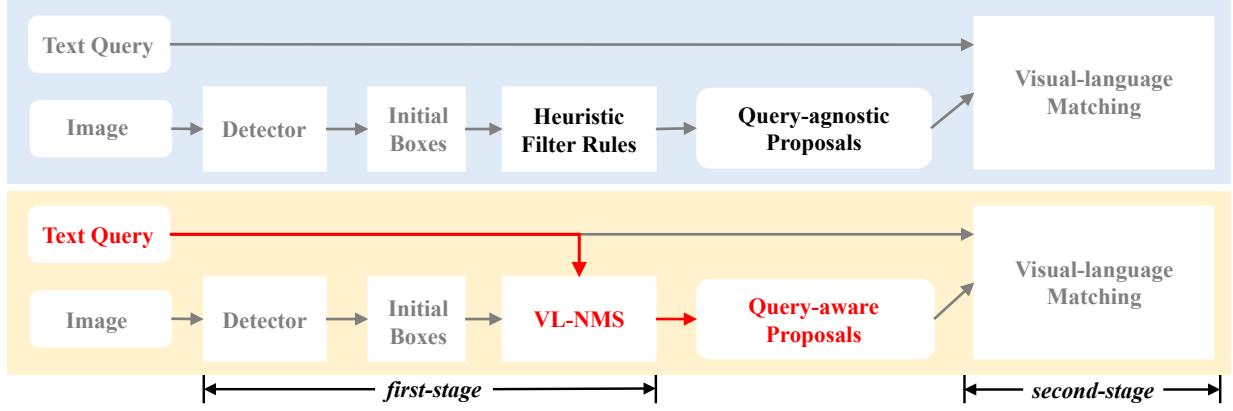


Fig. 4. Upper: A typical two-stage visual-language matching framework, which uses heuristic filter rules to obtain query-agnostic proposals at the first-stage. Below: The VL-NMS module can generate query-aware proposals by considering the text query at the first stage.

3) Heuristic-based [54, 55]: they dynamically adjust the thresholds for suppression according to some heuristic rules. In this paper, we are inspired by the criterion-based NMS, and design the VL-NMS, which uses both expression relatedness and detection confidence as the criterion.

### III. APPROACH

In this section, we first revisit the typical two-stage visual-language matching framework, and then introduce the details about VL-NMS, including the relatedness module, the ground-truth acquisition and the training objectives.

#### A. Revisiting Two-Stage Visual-language Matching

The two-stage framework is the most prevalent pipeline for visual-language matching tasks. As shown in Fig. 4, it consists of two separate stages: proposal generation at the first-stage and multimodal matching at the second-stage.

1) *Proposal Generation*: Given an image, current two-stage methods always resort to a well pre-trained detector to obtain a set of initially detected bboxes, and utilize an NMS operation to remove duplicate bboxes. However, even after the NMS operation, there are still thousands of bboxes left (e.g., for REG task, each image in RefCOCO has an average of 3,500 detections). To relieve the burden of the following multimodal matching step, all existing works further filter these bboxes based on their detection confidences. Although this heuristic filter rule can reduce the number of proposals, it also results in a drastic drop in the recall of the mentioned instances. Especially for the REG task, this recall drop can be fatal as the grounding process at the second stage will be guaranteed to fail if the referent is missed at the first stage. Detailed recall statistics of the referent and contextual objects on three REG benchmarks is reported in Table I.

2) *Multimodal Matching*: For the REG task, in the training phase, two-stage methods usually use the ground-truth regions in COCO as proposals, and the number is quite small (e.g., each image in RefCOCO has an average of 9.84 ground-truth regions). For explainable grounding, state-of-the-art two-stage grounding methods always compose these proposals into graph [56, 27] or tree [2, 25] structures. As the number

of proposals increases linearly, the number of computation increases exponentially. Therefore, in the test phase, it is a must for them to filter detections at the end of the first stage. For the ITM task, in both training and test phases, two-stage methods [4, 5, 6] normally utilize the bottom-up attention mechanism proposed in [13] and take a fix number of proposals as input at the second stage (normally 36 bboxes per image). Although this number is relatively large compared to REG, reducing the number of proposals can help improve the efficiency of the following image-sentence matching process and greatly shorten the retrieval time.

#### B. Relatedness Module

An overview of the VL-NMS model is shown in Fig. 5. The core of VL-NMS is the relatedness module. Given an image, a pre-trained detector can generate thousands of initial bboxes. To reduce the computation of the relatedness module, we first use a threshold  $\delta$  to filter the bboxes with classification confidence, and obtain a filtered bbox set  $\mathcal{B}$ . For each bbox  $b_i \in \mathcal{B}$ , we use a region visual encoder  $e_v$  (i.e., an RoI Pooling layer and a convolutional head network) to extract the bbox feature  $v_i \in \mathbb{R}^v$ . Meanwhile, for the text query  $Q$ , we use a text encoder  $e_q$  (i.e., a Bi-GRU) to output a set of word features  $\{w_1, \dots, w_{|Q|}\}$ , where  $w_j \in \mathbb{R}^q$  is the  $j$ -th word feature. For each bbox  $b_i$ , we use a soft-attention mechanism [57] to calculate a unique query feature  $q_i$  by:

$$\begin{aligned} v_i^a &= \text{MLP}_a(v_i), \quad a_{ij} = \text{FC}_s([v_i^a; w_j]), \\ \alpha_{ij} &= \text{softmax}_j(a_{ij}), \quad q_i = \sum_j \alpha_{ij} w_j, \end{aligned} \quad (1)$$

where  $\text{MLP}_a$  is a two-layer MLP mapping  $v_i \in \mathbb{R}^v$  to  $v_i^a \in \mathbb{R}^q$ ,  $\text{FC}_s$  is a FC layer to calculate the similarity between bbox feature  $v_i^a$  and word feature  $w_j$ , and  $[\cdot]$  is a concatenation operation. Then, we combine the features from both modalities and predict the relatedness score  $r_i$ :

$$\begin{aligned} v_i^b &= \text{MLP}_b(v_i), \quad m_i = \text{L2Norm}(v_i^b \odot q_i), \\ \hat{r}_i &= \text{FC}_r(m_i), \quad r_i = \text{sigmoid}(\hat{r}_i), \end{aligned} \quad (2)$$

where  $\text{MLP}_b$  is a two-layer MLP mapping  $v_i \in \mathbb{R}^v$  to  $v_i^b \in \mathbb{R}^q$ ,  $\odot$  is element-wise multiplication,  $\text{L2Norm}$  is  $l_2$  normalization, and  $\text{FC}_r$  is a FC layer mapping  $m_i \in \mathbb{R}^q$  to  $\hat{r}_i \in \mathbb{R}$ .



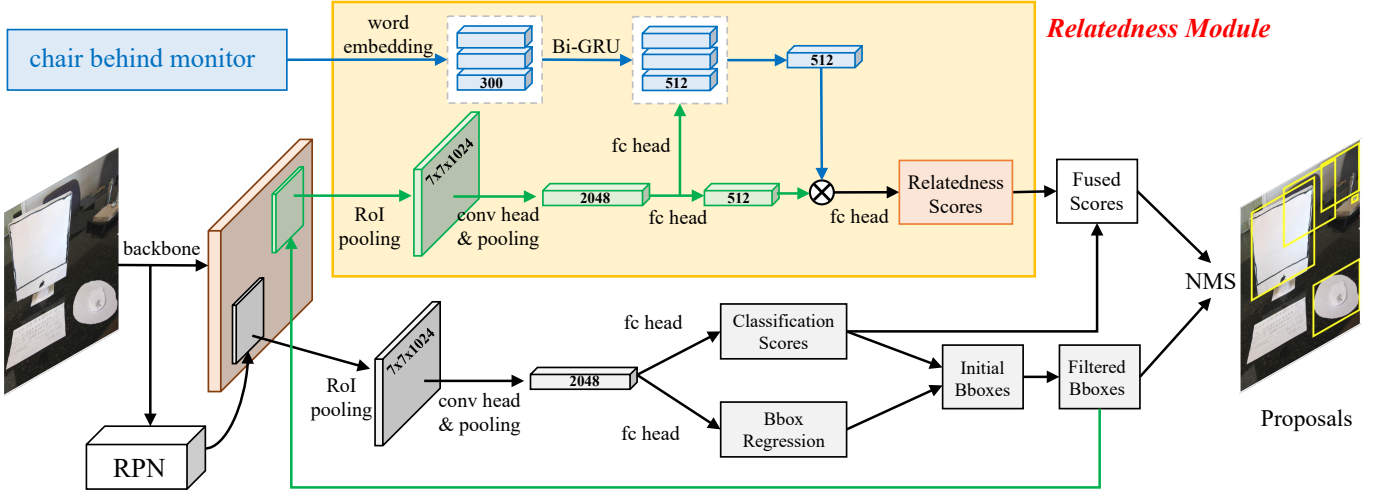


Fig. 5. The overview of VL-NMS model. Given an image, the model uses a pre-trained detector to generate thousands of initial bboxes. Then, the text query and hundreds of filtered bboxes with detection confidence beyond a threshold are fed into the relatedness module to predict the relatedness scores. Lastly, the relatedness scores are fused with detection confidences and the fused scores are used as the suppression criterion of NMS.

After obtaining the relatedness score  $r_i$  for bbox  $b_i$ , we multiply  $r_i$  with the classification confidence  $c_i$  for bbox  $b_i$  from the original detector, and utilize the product of two scores  $s_i$  as the suppression criterion of the NMS operation, i.e.,  $s_i = r_i \times c_i$ . We argue that fusing by multiplication is straightforward, doesn't introduce any extra hyper-parameters, and yields competing empirical results over other methods, such as weighted summarization.

### C. Acquisition of Ground-Truth Annotations

To learn the relatedness score for each bbox, we need the ground-truth annotations for all instances mentioned in the text query. However, both REG and ITM datasets don't contain such dense instance-level annotations, making it necessary to build pseudo ground-truth.

For the REG task, current datasets only have annotations about the referent. Thus, we need to generate pseudo ground-truths for contextual objects. Specifically, we explore two alternatives:

- **Text Similarity based Method.** We first assign POS tags to each word in the expression using the spaCy POS tagger and extract all nouns in the expression. Then, we calculate the cosine similarity between GloVe embeddings of extracted nouns and category names of ground-truth regions in COCO<sup>2</sup>. Lastly, we use threshold  $\gamma$  to filter regions as the pseudo ground-truths.
- **WSPG based Method.** To relieve two-stage REG methods from depending on COCO detection annotations, we propose to use a pretrained weakly supervised phrase grounding (WSPG) method to generate pseudo ground-truth for contextual objects. Note that the performance of WSPG methods is far from ideal. Hence directly using the results of a WSPG model as the first stage proposals is not feasible.

<sup>2</sup>Two-stage methods always use an object detector pretrained on COCO detection dataset. Thus, we don't use extra or more annotations.

In the training phase, we regard all the pseudo ground-truth bboxes and annotated referent bboxes as foreground bboxes.

For the ITM task, we can use annotations from phrase grounding datasets as our "golden" pseudo ground-truth. Alternatively, to relieve VL-NMS from using extra annotations from other tasks, we propose to transfer VL-NMS model pretrained on REG dataset to ITM task at inference time. Detailed measures and empirical results are described in the experiment section.

### D. Training Objectives for VL-NMS

We explored two types of training objectives.

1) **Binary XE Loss:** For each bbox  $b_i \in \mathcal{B}$ , if it has a high overlap (i.e.,  $\text{IoU} > 0.5$ ) with any foreground bbox, its ground-truth relatedness score  $r^*$  is set to 1, otherwise  $r^* = 0$ . Then the relatedness score prediction becomes a binary classification problem. We can use the binary cross-entropy (XE) loss as the training objective:

$$L = -\frac{1}{|\mathcal{B}|} \sum_{i=1}^{|\mathcal{B}|} r_i^* \log(r_i) + (1 - r_i^*) \log(1 - r_i). \quad (3)$$

2) **Ranking Loss:** Generally, if a bbox has a higher IoU with foreground bboxes, the relatedness between the bbox and expression should be higher, i.e., we can use the ranking loss as the training objectives:

$$L = \frac{1}{N} \sum_{(b_i, b_j), \rho_i < \rho_j} \max(0, r_i - r_j + \alpha), \quad (4)$$

where  $\rho_i$  denotes the largest IoU value between bbox  $b_i$  and foreground bboxes,  $N$  is the total number of pos-neg training pairs, and  $\alpha$  is a constant to control the ranking margin, set as 0.1. To select the pos-neg pair  $(b_i, b_j)$ , we follow the sampling-after-splitting strategy [50]. Specifically, we first divide the bbox set  $\mathcal{B}$  into 6 subsets based on a quantization  $q$ -value:  $q_i = \lceil \max(0, \rho_i - 0.5) / 0.1 \rceil$ , i.e., bboxes with higher IoU values will have larger  $q$ -values. Then, all bboxes with  $\rho > 0.5$  are selected as positive samples. For each positive

TABLE I  
RECALL (%) OF THE REFERENT AND CONTEXTUAL OBJECTS.

THE BASELINE DETECTOR IS A RESNET-101 BASED MASK R-CNN WITH PLAIN GREEDYNMS. ‘B’ DENOTES VL-NMS WITH BINARY XE LOSS, ‘R’ DENOTES VL-NMS WITH RANKING LOSS. ‘REAL’ DENOTES THE REAL CASE USED IN THE STATE-OF-THE-ART TWO-STAGE METHODS.

VL-NMS		Referent								Contextual Objects							
		RefCOCO			RefCOCO+			RefCOCOg		RefCOCO			RefCOCO+			RefCOCOg	
		val	testA	testB	val	testA	testB	val	test	val	testA	testB	val	testA	testB	val	test
N=100		97.60	97.81	96.58	97.79	97.78	96.99	97.18	96.91	90.14	89.85	90.53	89.53	88.47	90.69	90.56	90.30
	B	97.75	98.59	97.08	97.96	98.39	97.50	97.61	97.44	90.38	90.31	90.64	89.67	88.88	91.04	90.36	90.37
	R	97.62	98.02	96.78	97.71	98.06	97.14	97.18	97.08	90.22	89.83	90.63	89.70	88.62	90.71	90.67	90.30
Real		88.84	93.99	80.77	90.71	94.34	84.11	87.83	87.88	74.97	78.60	70.19	76.34	77.45	73.52	75.69	75.87
	B	<b>92.51</b>	<b>95.56</b>	<b>88.28</b>	<b>93.42</b>	<b>95.86</b>	<b>88.95</b>	<b>90.28</b>	<b>90.34</b>	<b>78.75</b>	<b>80.14</b>	<b>76.47</b>	<b>78.44</b>	<b>78.82</b>	<b>77.49</b>	76.12	76.57
	R	90.50	94.75	83.87	91.62	95.14	86.42	89.01	88.96	76.79	79.12	72.99	77.66	78.44	75.59	<b>76.68</b>	<b>76.73</b>

sample, we rank all bboxes with smaller  $q$ -value based on the predicted relatedness scores and select the top- $h$  bboxes as negative samples.

We empirically find that training with binary XE loss is more robust while training with ranking loss has the advantage of explicitly enforcing ranks within proposals and sometimes yields better results.

#### IV. EXPERIMENTS

##### A. Results on Referring Expression Grounding

**Datasets.** We evaluate VL-NMS on three challenging REG benchmarks: 1) **RefCOCO** [18]: It consists of 142,210 referring expressions for 50,000 objects in 19,994 images. These expressions are collected in an interactive game interface [58], and the average length of each expression is 3.5 words. All expression-referent pairs are split into train, val, testA, and testB sets. The testA set contains images with multiple people and the testB set contains images with multiple objects. 2) **RefCOCO+** [18]: It consists of 141,564 referring expressions for 49,856 objects in 19,992 images. Similar to RefCOCO, these expressions are collected from the same game interface, and have train, val, testA, and testB splits. But different from RefCOCO, these expressions don’t include absolute location of the referent. 3) **RefCOCOg** [11]: It consists of 104,560 referring expressions for 54,822 objects in 26,711 images. These expressions are collected in a non-interactive way, and the average length of each expression is 8.4 words. Compared to RefCOCO and RefCOCO+, expressions in RefCOCOg are more descriptive and generally involve more objects and relations. We follow the same split as [59].

**Evaluation Metrics.** For the REC task, we use top-1 accuracy as evaluation metric. When the IoU between the predicted and ground truth is larger than 0.5, the prediction is considered to be correct. For the RES task, we use the overall IoU and Pr@X (the percentage of samples with IoU higher than X)<sup>3</sup> as metrics.

**Implementation Details.** We build a vocabulary for each dataset by filtering out the words less than 2 times, and exploit the 300-d GloVe embeddings as the initialization of word embeddings. We use an “unk” symbol to replace all words

out of the vocabulary. The largest length of sentences is set to 10 for RefCOCO and RefCOCO+, 20 for RefCOCOg. The text encoder  $e_q$  is a bidirectional GRU with a hidden size of 256. For the visual encoder  $e_v$ , we use the same head network of the Mask R-CNN with ResNet-101 backbone<sup>4</sup> as prior works [1], and utilize the pre-trained weights as initialization. The weights of the original detector (*i.e.*, the gray part in Figure 5) are fixed during training. The whole model is trained with Adam optimizer. The learning rate is initialized to  $4e-4$  for the head network and  $5e-3$  for the rest of network. We use a batch size of 8. The thresholds  $\delta$  and  $\gamma$  are set to 0.05 and 0.4, respectively. For the ranking loss, the top- $h$  is set to 100. We build pseudo ground-truth based on text similarity, if not mentioned otherwise.

1) *Recall Analyses of Critical Objects:* To evaluate the effectiveness of the VL-NMS in improving the recall of both referent and contextual objects, we compare VL-NMS with plain GreedyNMS used in the baseline detector (*i.e.*, ResNet-101 based Mask R-CNN). Since we only have annotated ground-truth bboxes for the referent, we calculate the recall of pseudo ground-truths to approximate the recall of contextual objects. The results are reported in Table I, and more detailed results are provided in the supplementary materials. From Table I, we have the following observations. When using top-100 bboxes as proposals, all three methods can achieve near-perfect recall ( $\approx 97\%$ ) for the referent and acceptable recall ( $\approx 90\%$ ) for the contextual objects, respectively. However, as the number of proposals decreases to a very small number (*e.g.*,  $< 10$  in the real case), the recall of the baseline all drops significantly (*e.g.*, 15.81% for the referent and 20.34% for the contextual objects on RefCOCO testB). In contrast, VL-NMS can help narrow the gap over all dataset splits. Especially, the improvement is more obvious on the testB set (*e.g.*, 7.51% and 4.85% absolute gains for the recall of referent on RefCOCO and RefCOCO+), where the categories of referents are more diverse and the recalls are relatively lower.

2) *Architecture Agnostic Generalization:* Since the VL-NMS model is agnostic to the second stage network, it can be easily integrated into any referent grounding architectures. To evaluate the effectiveness and generalizability of VL-NMS in boosting the grounding performance of different backbones,

<sup>3</sup>Due to the limited space, all RES results with the Pr@X metric are provided in the supplementary materials.

<sup>4</sup><https://github.com/lichengunc/mask-faster-rcnn>

TABLE II

PERFORMANCE OF VL-NMS ON REC AND RES WITH DIFFERENT GROUNDING BACKBONES.

THE METRIC IS TOP-1 ACCURACY (%) FOR REC AND OVERALL IOU (%) FOR RES. ALL BASELINES USE THE RESNET-101 BASED MASK R-CNN AS FIRST-STAGE NETWORKS. THE BEST AND SECOND BEST METHODS UNDER EACH SETTING ARE MARKED IN BOLD AND ITALIC FONTS, RESPECTIVELY.

† DENOTES THE RESULTS ARE FROM OUR IMPLEMENTATIONS.

Models	Referring Expression Comprehension									Referring Expression Segmentation								
	RefCOCO			RefCOCO+			RefCOCOg			RefCOCO			RefCOCO+			RefCOCOg		
	val	testA	testB	val	testA	testB	val	test		val	testA	testB	val	testA	testB	val	test	
MAttNet [1]	76.65	81.14	69.99	65.33	71.62	56.02	66.58	67.27	56.51	62.37	51.70	46.67	52.39	40.08	47.64	48.61		
MAttNet†	76.92	81.19	69.58	65.90	<b>71.53</b>	57.23	67.52	67.55	57.14	62.34	51.48	47.30	<b>52.37</b>	41.14	48.28	49.01		
+VL-NMS B	<b>78.82</b>	<b>82.71</b>	<b>73.94</b>	<b>66.95</b>	71.29	<b>58.40</b>	68.89	<b>68.67</b>	<b>59.75</b>	<b>63.48</b>	<b>55.66</b>	<b>48.39</b>	51.57	<b>42.56</b>	49.54	<b>50.38</b>		
+VL-NMS R	77.98	82.02	71.64	66.64	71.36	58.01	<b>69.16</b>	67.63	58.32	62.96	53.68	47.87	51.85	41.41	<b>50.13</b>	49.07		
NMTree [2]	76.41	81.21	70.09	66.46	72.02	57.52	65.87	66.44	56.59	63.02	52.06	47.40	53.01	41.56	46.59	47.88		
NMTree†	76.54	81.32	69.66	66.65	71.48	57.74	65.65	65.94	56.99	62.88	51.90	47.75	52.36	41.86	46.19	47.41		
+VL-NMS B	<b>78.67</b>	<b>82.09</b>	<b>73.78</b>	<b>67.15</b>	71.76	58.70	<b>67.30</b>	<b>66.93</b>	<b>59.95</b>	<b>63.25</b>	<b>55.64</b>	<b>48.68</b>	52.30	<b>42.64</b>	<b>48.14</b>	<b>48.59</b>		
+VL-NMS R	77.81	81.69	71.78	67.03	<b>71.78</b>	<b>58.79</b>	66.81	66.31	58.42	62.69	53.60	48.27	<b>52.65</b>	42.18	47.72	48.09		
CM-A-E [3]	78.35	83.14	71.32	68.09	73.65	58.03	67.99	68.67	—	—	—	—	—	—	—	—		
CM-A-E†	78.35	83.12	71.32	68.19	73.04	58.27	69.10	69.20	58.23	64.60	53.14	49.65	<b>53.90</b>	41.77	49.10	50.72		
+VL-NMS B	<b>80.70</b>	<b>84.00</b>	<b>76.04</b>	68.25	<b>73.68</b>	<b>59.42</b>	<b>70.55</b>	<b>70.62</b>	<b>61.46</b>	<b>65.55</b>	<b>57.41</b>	49.76	53.84	<b>42.66</b>	<b>51.21</b>	<b>51.90</b>		
+VL-NMS R	79.55	83.58	73.62	<b>68.51</b>	73.14	58.38	69.77	70.01	59.72	64.87	55.63	<b>49.86</b>	52.62	41.87	50.13	51.44		

we incorporate VL-NMS into three state-of-the-art two-stage grounding methods: **MAttNet** [1], **NMTree** [2], and **CM-A-E** [3]. All results are reported in Table II. From Table II, we can observe that both variants of VL-NMS can consistently improve the grounding performance of all three backbones on both REC and RES. The improvement is more significant on the testB set (*e.g.*, 4.72% and 3.23% absolute performance gains for CM-A-E in REC and RES), which meets our expectation, *i.e.*, the improvements of the recall of critical objects at the first stage have a strong positive correlation with the improvements of grounding performance at the second stage. Comparing between the two variants of VL-NMS, in most of cases, VL-NMS B achieves better grounding performance. We argue that this performance difference may come from the imbalanced nature of positive and negative samples in each ranking level during the training of VL-NMS R.

3) *Comparison with State-of-the-Arts*: We incorporate VL-NMS with binary XE loss into CM-A-E model, dubbed **CM-A-E+VL-NMS**, and compare it against state-of-the-art REC and RES methods. For fair comparison, we group state-of-the-art REC methods into: 1) two-stage methods: **VC** [60], **ParalAttn** [61], **LGRANs** [27], **DGA** [56], **NMTree** [2], **MAttNet** [1], **RvG-Tree** [25], and **CM-A-E** [3]; 2) one-stage methods: **SSG** [29], **FAOA** [30], **RCCF** [31], and **RSC-Large** [33]. Analogously, we group state-of-the-art RES methods into: 1) two-stage methods: **MAttNet** [1], **NMTree** [2], and **CM-A-E** [3]; 2) one-stage methods: **STEP** [35], **BRINet** [38], **CMPC** [36], and **MCN** [32]. The results are reported in Table III. For the REC task, CM-A-E+VL-NMS achieves a new record-breaking performance that is superior to all existing REC methods on three benchmarks. Specifically, VL-NMS improves the strong baseline CM-A-E with an average of 2.64%, 0.53%, and 2.26% absolute performance gains on RefCOCO, RefCOCO+, and RefCOCOg. For the RES task, CM-A-E+VL-NMS achieves a new state-of-the-art performance of two-stage methods over most of the dataset splits.

TABLE III

COMPARISON WITH STATE-OF-THE-ART MODELS ON REC AND RES. THE METRIC IS TOP-1 ACCURACY (%) FOR REC AND OVERALL IOU (%) FOR RES. † DENOTES THE RESULTS ARE FROM OUR IMPLEMENTATION.

Models		RefCOCO		RefCOCO+		RefCOCOg test
		testA	testB	testA	testB	
Referring Expression Comprehension						
one-s.	SSG [29]	76.51	67.50	62.14	49.27	—
	FAOA [30]	74.88	66.32	61.89	49.46	58.90
	RCCF [31]	81.06	71.85	70.35	56.32	65.73
	RSC-Large [33]	80.45	72.30	68.36	67.30	67.20
two-s.	VC [60]	73.33	67.44	58.40	53.18	—
	ParalAttn [61]	75.31	65.52	61.34	50.86	—
	LGRANs [27]	76.60	66.40	64.00	53.40	—
	DGA [56]	78.42	65.53	69.07	51.99	63.28
	NMTTree [2]	74.81	67.34	61.09	53.45	61.46
	MAttNet [1]	81.14	69.99	71.62	56.02	67.27
	RvG-Tree [25]	78.61	69.85	67.45	56.66	66.51
	NMTTree [2]	81.21	70.09	72.02	57.52	66.44
	CM-A-E [3]	83.14	71.32	73.65	58.03	68.67
	CM-A-E+VL-NMS	84.00	76.04	73.68	59.42	70.62
Referring Expression Segmentation						
one-s.	STEP [35]	63.46	57.97	52.33	40.41	—
	BRINet [38]	62.99	59.21	52.32	42.41	—
	CMPC [36]	64.53	59.64	53.44	43.23	—
	MCN [32]	64.20	59.71	54.99	44.69	49.40
two-s.	MAttNet [1]	62.37	51.70	52.39	40.08	48.61
	NMTTree [2]	63.02	52.06	53.01	41.56	47.88
	CM-A-E <sup>†</sup> [3]	64.60	53.14	53.90	41.77	50.72
	CM-A-E+VL-NMS	65.55	57.41	53.84	42.66	51.90

Similarly, VL-NMS improves CM-A-E with an average of 2.82%, 0.31%, and 1.65% absolute performance gains on three benchmarks. Note that since one-stage and two-stage RES models are pretrained on different datasets, the comparison between them is not strictly fair.

4) *Ablation Studies of Pseudo Ground-truth*: To validate the effectiveness of pseudo ground-truth, we further compare VL-NMS with a strong baseline: VL-NMS without pseudo

TABLE IV

ABLATION STUDIES OF TEXT SIMILARITY BASED PSEUDO GROUND-TRUTH ON REC TASK. THE GROUNDING BACKBONE IS CM-A-E.

VL-NMS	RefCOCO		RefCOCO+		RefCOCOg test
	testA	testB	testA	testB	
w/o Pseudo GT	83.63	<b>76.09</b>	71.83	58.64	68.76
w/ Pseudo GT	<b>84.00</b>	76.04	<b>73.68</b>	<b>59.42</b>	<b>70.62</b>

TABLE V

EFFECTIVENESS OF WEAKLY SUPERVISED PHRASE GROUNDING BASED PSEUDO GROUND-TRUTH ON REC TASK. TO AVOID USING COCO ANNOTATIONS, ALL BASELINES USE FASTER R-CNN PRETRAINED ON VISUAL GENOME DATASET [13] AS FIRST-STAGE NETWORKS.

Models	RefCOCO		RefCOCO+		RefCOCOg test
	testA	testB	testA	testB	
MAttNet [1]	45.87	51.64	45.60	44.45	45.33
+VL-NMS-WSPG	<b>77.67</b>	<b>70.11</b>	<b>68.84</b>	<b>56.09</b>	<b>64.60</b>
+VL-NMS-COCO	77.92	70.70	68.93	56.33	64.85
NMTTree [2]	46.72	51.03	46.02	44.43	44.59
+VL-NMS-WSPG	<b>77.16</b>	<b>69.30</b>	<b>69.09</b>	<b>55.86</b>	<b>64.19</b>
+VL-NMS-COCO	77.43	69.28	69.46	55.12	64.26
CM-A-E [3]	48.06	52.74	48.01	45.76	46.29
+VL-NMS-WSPG	<b>79.97</b>	<b>72.56</b>	<b>69.87</b>	<b>55.61</b>	<b>66.03</b>
+VL-NMS-COCO	80.06	72.68	70.24	56.29	66.03

ground-truth. The results are shown in Table IV. Both methods are trained with the same set of hyper-parameters and tested with CM-A-E as grounding backbone. We can observe that VL-NMS performs better on all splits except RefCOCO testB where the performance difference between the two methods is trivial (0.05%). Especially on RefCOCOg dataset where the expressions are more complex, training with pseudo ground-truth lifts the performance by 1.8%. These results validate the effectiveness of using pseudo ground-truth for contextual objects in the training phase. Meanwhile, from another perspective, VL-NMS trained without pseudo ground-truth can be regarded as a one-stage REC model, which suggests that current one-stage REC methods, trained to yield the referent instead of all critical objects, are not as qualified as VL-NMS for generating proposals for two-stage REG methods.

5) *Grounding without COCO Annotations*: As all three REG benchmarks are built upon COCO dataset, most state-of-the-art grounding methods, either explicitly or implicitly, make use of extra COCO annotations. Two-stage methods normally use a COCO pretrained detector to extract proposals at the first stage while one-stage methods utilize the pretrained detector weights as initialization of backbone networks. In VL-NMS, we also use COCO annotations to build pseudo ground-truth for contextual objects using the text similarity based method. To relieve two-stage REG framework from depending on extra data, here we make an attempt to remove COCO detection annotations (*i.e.* ground-truth bboxes and categories) from the grounding pipeline. Firstly, we replace the COCO pretrained detector at the first stage with a widely used Visual Genome pretrained detector [13]. Secondly, we propose an alternative way to build pseudo ground-truth for contextual objects by means of weakly supervised phrase grounding

TABLE VI

INFERENCE TIME OF TWO-STAGE GROUNDING PIPELINE WITH VL-NMS. MEASURED ON A SINGLE NVIDIA 1080Ti.

First Stage		Second Stage	
res101-mrcnn	<b>VL-NMS</b>	MAttNet	NMTTree
0.1893	0.0974	0.4002	0.4058

(WSPG). Specifically, we use a pretrained state-of-the-art WSPG model [47] to ground all noun chunks in the expression and take the localization results as pseudo ground-truth. Then we regard all pseudo ground-truth bboxes and the annotated referent bbox as foreground bboxes to train VL-NMS. The results are shown in Table V. We can observe that replacing the COCO pretrained detector results in a much inferior grounding performance compared to Table II (*e.g.*, performance of CM-A-E decreases by 35.94%). Applying VL-NMS with WSPG-based pseudo ground-truth can consistently and greatly boost the performance of all baselines over three REG benchmarks (*e.g.*, performance of CM-A-E increases by 31.91%, almost as high as original CM-A-E+VL-NMS in Table II). We also compared the two ways of generating pseudo ground-truth. As expected, text similarity based method (dubbed VL-NMS-COCO) generally yields superior results over WSPG based methods (dubbed VL-NMS-WSPG) by exploiting COCO bbox and category annotations. But the performance gap between these two methods is negligible.

6) *Inference Time of VL-NMS*: As VL-NMS needs to forward the detected bboxes of a Mask RCNN back through the RoI pooling layer to calculate the relatedness score, it is reasonable to concern about the added time complexity of VL-NMS. We quantitatively measured the inference time of each component of two-stage grounding pipeline with VL-NMS. As shown in Table VI, the inference time of VL-NMS is marginal ( $\approx 16\%$  extra time for both MAttNet and NMTTree).

## B. Results on Image-Text Matching

**Datasets.** We evaluate VL-NMS on one widely used ITM benchmark: Flickr30k [62]. It consists of 31,000 images collected from Flickr, each associated with five human annotated captions. Following the split in [4], we use 1,000 images for validation, 1,000 images for testing and the rest for training.

**Evaluation Metrics.** Following [4], we adopt Recall@K (R@K) to measure the performance of bidirectional retrieval, namely retrieving sentence with image query (sentence retrieval) and retrieving image with sentence query (image retrieval). R@K is defined as the fraction of queries for which the correct item is retrieved in the top-k scoring items. Also, to evaluate the overall retrieval performance, we report the R@Sum metric which is the sum of all R@K metrics as in [5].

**Settings.** To train VL-NMS, we need bbox annotations for all critical objects mentioned by the text query. However, ITM datasets don't provide such instance level annotations. To address this issue, we explore two alternatives to apply VL-NMS on ITM task: 1) *By using extra annotations (VL-NMS-GT)*: We borrow bbox annotations from Flickr30k Entities, which is a phrase grounding dataset built upon Flickr30k, as



TABLE VII  
PERFORMANCE OF VL-NMS ON ITM TASK WITH DIFFERENT MATCHING BACKBONES. THE METRICS ARE RECALL@K (%) AND RECALL@SUM(%).  
THE BEST AND SECOND BEST METHODS UNDER EACH SETTING ARE MARKED IN BOLD AND ITALIC FONTS, RESPECTIVELY.

	Models	Sentence Retrieval			Image Retrieval			R@sum
		R@1	R@5	R@10	R@1	R@5	R@10	
$N=36$	SCAN [4]	66.1	88.5	94.0	44.6	74.4	83.2	450.8
	+VL-NMS-GT	<b>70.0</b>	<b>90.8</b>	<b>95.0</b>	<b>46.6</b>	<b>75.2</b>	<b>84.1</b>	<b>461.7</b>
	+VL-NMS-Transfer	67.5	88.7	94.3	46.1	74.9	83.3	454.8
	IMRAM [5]	<b>68.7</b>	91.2	95.6	50.0	<b>77.8</b>	<b>85.3</b>	<b>468.6</b>
	+VL-NMS-GT	67.3	91.7	<b>96.0</b>	49.5	77.3	85.1	466.9
	+VL-NMS-Transfer	67.4	<b>91.9</b>	95.9	<b>50.4</b>	77.0	85.0	467.6
$N=10$	SCAN [4]	57.8	83.1	90.1	40.8	68.6	78.1	418.5
	+VL-NMS-GT	<b>65.4</b>	<b>86.6</b>	<b>91.9</b>	<b>42.9</b>	<b>71.0</b>	79.7	<b>437.5</b>
	+VL-NMS-Transfer	61.1	86.6	91.5	41.7	70.5	<b>79.8</b>	431.2
	IMRAM [5]	49.8	78.3	87.5	34.2	62.9	72.9	385.6
	+VL-NMS-GT	<b>67.8</b>	<b>87.6</b>	<b>93.0</b>	<b>44.5</b>	<b>71.7</b>	80.1	<b>444.7</b>
	+VL-NMS-Transfer	59.9	85.2	91.2	42.8	71.5	<b>80.6</b>	431.2

golden ground-truth for critical objects. This can serve as the performance upper bound for VL-NMS on ITM task. 2) *By means of transfer learning (VL-NMS-Transfer)*: Given image-sentence pairs from ITM dataset, we directly use a VL-NMS model trained on REG dataset to generate proposals at the first stage. Specifically, we choose RefCOCOg as source dataset as it contains longer expressions which is closer to the captions in Flickr30k. We make this attempt in the belief that the fine-grained correspondence between image regions and text words learned by VL-NMS is fundamental and hence transferable. We experiment with using different number of proposals at the second stage, namely 36 proposals per image which is the default case in baseline methods and 10 proposals per image which is faster and requires less memory.

**Baselines.** We incorporate VL-NMS into two state-of-the-art two-stage ITM methods: **SCAN** [4] and **IMRAM** [5]. Specifically, we use the SCAN i-t AVG model with default configuration and Full-IMRAM with single matching step due to memory constraint.

**Results.** As is shown in Table VII, when using SCAN as backbone, no matter how many proposals are used at the second stage, both VL-NMS-GT and VL-NMS-Transfer can consistently improve the matching performance. VL-NMS-GT generally has higher performance lift as bbox annotations from phrase grounding are used during training. When using IMRAM as backbone with 36 proposals per image, the matching results are mixed. We attribute this to the fact that IMRAM is more complex and stronger so that 36 proposals are more than enough for IMRAM to extract necessary visual information from images. When reducing the number of proposals to 10, the performance of IMRAM drops drastically (-83% on R@sum metric), which suggests that complex ITM methods are more sensitive to inferior proposals. Applying both versions of VL-NMS can help capture meaningful visual context with limited number of proposals, resulting in a huge performance boost over baseline (+59.1% for VL-NMS-GT and +45.6% for VL-NMS-Transfer on R@sum metric).

### C. Qualitative Results

We illustrate the qualitative results between CM-A-E+VL-NMS and baseline CM-A-E on REC and RES task in Figure 6. From the results in line (b), we can observe that VL-NMS can assign high attention weights to words that are more relevant to individual referents (*e.g.*, umbrella, man, and zebra). The results in line (c) show that the generated pseudo ground-truth bboxes can almost contain all contextual objects in the expression, except a few objects whose categories are far different from the categories of COCO (*e.g.*, sweater, armrest, and grass). By comparing the results between line (d) and line (f), we have the following observations: 1) The baseline method tends to detect more false-positive proposals (*i.e.*, the blue bboxes), and misses some critical objects (*i.e.*, the red and green bboxes). Instead, VL-NMS can generate expression-aware proposals which are more relevant to the expression. 2) Even for the failure cases of CM-A-E+VL-NMS (*i.e.*, the last two columns), VL-NMS still generates more reasonable proposals (*e.g.*, with less false positive proposals), and the grounding errors mainly come from the second stage grounding model. The segmentation results of the two methods are shown in line (e) and line (g). We can observe that when extending REC models to RES task, the quality of the segmentation mask is heavily dependent on the precision of REC predictions. If the REC model can ground the referent precisely with a bbox, the downstream segmentation branch can segment the referent from the bbox almost perfectly. Thus, by lifting the grounding precision of two-stage REC methods, VL-NMS can also help to improve the performance of two-stage RES methods.

## V. CONCLUSIONS AND FUTURE WORKS

In this paper, we focused on the two-stage visual-language grounding and matching, and discussed the overlooked mismatch problem between the roles of proposals in different stages. Particularly, we proposed a novel algorithm VL-NMS to calibrate this mismatch. VL-NMS tackles the problem by considering the query at the first stage, and learns a relatedness



Fig. 6. Qualitative REC and RES results on RefCOCOg showing comparisons between correct (green tick) and wrong referent grounds (red cross) by CM-A-E and CM-A-E+VL-NMS. (a): The referring expression and input image. (b): The visualization of word attention weights  $\alpha$  (cf., Eq. (1)) for each referent object. (c): The annotated ground-truth bbox of the referent (marked in red) and the generated pseudo ground-truth bboxes of the contextual objects (marked in green). (d): The upper row demonstrates the proposals generated by an off-the-shelf object detector and the REC predictions of the downstream CM-A-E[3]; the lower row demonstrates the two-stage RES predictions acquired using the REC predictions from the upper row, the detailed method of which is fully described in [1]. (e): VL-NMS proposals, the REC and RES predictions from the downstream CM-A-E, arranged in the same format as (d). The predicted bbox in REC is shown in dashed line. The denotations of bbox colors are as follows. **Red**: The bbox hits (IoU>0.5) the ground-truth bbox of the referent; **Green**: The bbox hits one of the pseudo ground-truth bboxes of the contextual objects; **Blue**: The false positive proposals.

score between each detected proposal and the query. The product of the relatedness score and classification score serves as the suppression criterion for the NMS operation. Meanwhile, VL-NMS is agnostic to the downstream grounding and matching step, hence can be integrated into any SOTA two-stage grounding and matching methods. Extensive ablations on

various tasks and benchmarks consistently demonstrate that VL-NMS is robust, generalizable and transferable. Moving forward, we plan to apply VL-NMS into other proposal-drive visual-language tasks which suffer from the same mismatch issue, e.g., video grounding [63, 64] and VQA [65].

# APPENDIX A DETAILED RECALL OF REFERENT AND CONTEXTUAL OBJECTS

Detailed recall of referent and contextual objects are reported in Table VIII. As we can see, both two variants of VL-NMS can help boost the recall of the referent on all dataset splits. More specifically, VL-NMS B consistently achieves the best recall under all settings. Analogously, two variants can also improve the recall of contextual objects. However, for the contextual objects, it's hard to pick a winner between the two variants but it's safe to say that the best recall is always achieved by either of them. In conclusion, these results concretely validate the effectiveness of the proposed VL-NMS in boosting the recall of the referent and contextual objects.

TABLE VIII  
RECALL (%) OF REFERENT AND CONTEXTUAL OBJECTS WITH DIFFERENT  
NUMBERS OF PROPOSALS.

#	Model	RefCOCO		RefCOCO+		RefCOCOg
		testA	testB	testA	testB	test
Referent						
100	Baseline	97.81	96.58	97.78	96.99	96.91
	+ VL-NMS B	<b>98.59</b>	<b>97.08</b>	<b>98.39</b>	<b>97.50</b>	<b>97.44</b>
	+ VL-NMS R	98.02	96.78	98.06	97.14	97.08
50	Baseline	97.14	95.11	97.15	95.56	95.53
	+ VL-NMS B	<b>97.91</b>	<b>95.56</b>	<b>97.73</b>	<b>96.26</b>	<b>96.20</b>
	+ VL-NMS R	97.21	95.51	97.22	96.13	95.67
20	Baseline	95.85	91.44	95.90	91.92	92.96
	+ VL-NMS B	<b>96.89</b>	<b>92.86</b>	<b>96.65</b>	<b>93.56</b>	<b>94.25</b>
	+ VL-NMS R	96.32	91.93	96.37	92.66	93.19
10	Baseline	93.94	86.95	94.04	87.58	89.15
	+ VL-NMS B	<b>95.63</b>	<b>89.79</b>	<b>95.72</b>	<b>89.79</b>	<b>91.19</b>
	+ VL-NMS R	94.73	88.68	94.81	89.51	90.20
Real	Baseline	93.99	80.77	94.34	84.11	87.88
	+ VL-NMS B	<b>95.56</b>	<b>88.28</b>	<b>95.86</b>	<b>88.95</b>	<b>90.34</b>
	+ VL-NMS R	94.75	83.87	95.14	86.42	88.96
Contextual Objects						
100	Baseline	89.85	90.53	88.47	90.69	90.30
	+ VL-NMS B	<b>90.31</b>	<b>90.64</b>	<b>88.88</b>	<b>91.04</b>	<b>90.37</b>
	+ VL-NMS R	89.83	90.63	88.62	90.71	90.30
50	Baseline	88.37	88.78	86.90	88.85	88.25
	+ VL-NMS B	88.45	88.51	<b>87.62</b>	88.74	<b>88.36</b>
	+ VL-NMS R	<b>88.57</b>	<b>88.81</b>	87.15	<b>89.15</b>	88.34
20	Baseline	84.74	84.18	82.67	84.32	84.17
	+ VL-NMS B	<b>85.39</b>	83.81	<b>83.47</b>	83.74	<b>84.40</b>
	+ VL-NMS R	85.01	<b>84.21</b>	83.12	<b>84.73</b>	84.24
10	Baseline	76.56	76.79	73.76	77.02	78.37
	+ VL-NMS B	<b>80.24</b>	77.38	<b>77.84</b>	77.17	<b>79.07</b>
	+ VL-NMS R	78.87	<b>77.57</b>	76.30	<b>78.39</b>	79.05
Real	Baseline	78.60	70.19	77.45	73.52	75.87
	+ VL-NMS B	<b>80.14</b>	<b>76.47</b>	<b>78.82</b>	<b>77.49</b>	76.57
	+ VL-NMS R	79.12	72.99	78.44	75.59	<b>76.73</b>

# APPENDIX B DETAILED RES RESULTS WITH PR@X METRIC

The detailed RES results with Pr@X metric on RefCOCO, RefCOCO+ and RefCOCOg are shown in Table IX, Table X and Table XI respectively. We can observe that the VL-NMS can consistently improve the grounding performance of all baselines and dataset splits over most of the metric thresholds. In particular, it is worth noting that the VL-NMS significantly outperforms the baselines on RefCOCO testB split, RefCOCO+ testB split, where the category of the referent is more diverse, and on all splits of RefCOCOg, where the referring expressions are more complex. We attribute these performance gains to the richer contextual information conserved in the proposals generated by VL-NMS, which is consistent with our motivation.

# APPENDIX C MORE QUALITATIVE RESULTS ON REFCOCO AND REFCOCO+

Qualitative results including the comparisons of proposals between the baseline (*i.e.*, CM-A-E) and CM-A-E+VL-NMS as well as the visualization of REC and RES predictions on RefCOCO and RefCOCO+ are illustrated in Figure 7 and Figure 8, respectively.

From these qualitative results, we have the following observations: 1) The generated pseudo ground-truth bboxes can almost contain all contextual objects in the expression. 2) The baseline model tends to detect more false-positive proposals, and misses some critical objects. 3) Even in the failed cases on CM-A-E+VL-NMS, VL-NMS still generates express-aware proposals, and the grounding errors mainly come from the referent grounding step (*i.e.*, the second stage).

# REFERENCES

- [1] L. Yu, Z. Lin, X. Shen, J. Yang, X. Lu, M. Bansal, and T. L. Berg, "Mattnet: Modular attention network for referring expression comprehension," in *CVPR*, 2018.
- [2] D. Liu, H. Zhang, F. Wu, and Z.-J. Zha, "Learning to assemble neural module tree networks for visual grounding," in *ICCV*, 2019.
- [3] X. Liu, Z. Wang, J. Shao, X. Wang, and H. Li, "Improving referring expression grounding with cross-modal attention-guided erasing," in *CVPR*, 2019.
- [4] K.-H. Lee, X. Chen, G. Hua, H. Hu, and X. He, "Stacked cross attention for image-text matching," in *ECCV*, 2018.
- [5] H. Chen, G. Ding, X. Liu, Z. Lin, J. Liu, and J. Han, "Imram: Iterative matching with recurrent attention memory for cross-modal image-text retrieval," in *CVPR*, 2020.
- [6] C. Liu, Z. Mao, T. Zhang, H. Xie, B. Wang, and Y. Zhang, "Graph structured network for image-text matching," in *CVPR*, 2020.
- [7] F. Feng, X. Wang, and R. Li, "Cross-modal retrieval with correspondence autoencoder," in *ACM MM*, 2014.
- [8] S. Antol, A. Agrawal, J. Lu, M. Mitchell, D. Batra, C. Lawrence Zitnick, and D. Parikh, "Vqa: Visual question answering," in *ICCV*, 2015.
- [9] H. Chen, A. Suhr, D. Misra, N. Snavely, and Y. Artzi, "Touchdown: Natural language navigation and spatial reasoning in visual street environments," in *CVPR*, 2019.
- [10] J. Kim, T. Misu, Y.-T. Chen, A. Tawari, and J. Canny, "Grounding human-to-vehicle advice for self-driving vehicles," in *CVPR*, 2019.

TABLE IX  
RES PERFORMANCE (%) OF DIFFERENT ARCHITECTURES WITH PR@X METRIC ON REFCOCO. † DENOTES THAT THE RESULTS ARE FROM OUR REIMPLEMENTATION USING OFFICIAL RELEASED CODES.

Models	val					testA					testB				
	0.5	0.6	0.7	0.8	0.9	0.5	0.6	0.7	0.8	0.9	0.5	0.6	0.7	0.8	0.9
MAttNet [1]†	75.49	72.80	67.95	54.92	16.83	79.46	77.71	72.69	58.85	<b>13.79</b>	68.62	64.99	59.76	48.71	20.82
+VL-NMS B	<b>77.16</b>	<b>74.27</b>	<b>69.00</b>	55.74	<b>17.24</b>	<b>80.78</b>	<b>78.72</b>	73.50	<b>58.94</b>	13.72	<b>71.78</b>	<b>68.24</b>	<b>62.26</b>	49.81	21.28
+VL-NMS R	76.55	73.73	68.75	<b>55.79</b>	17.19	80.43	78.40	<b>73.66</b>	58.33	13.77	70.19	66.85	61.57	<b>51.01</b>	<b>21.77</b>
NMTTree [2]†	75.15	72.45	67.58	54.45	16.59	79.58	77.73	72.74	<b>58.87</b>	<b>13.88</b>	68.64	65.10	60.02	49.17	21.35
+VL-NMS B	<b>77.13</b>	<b>74.04</b>	<b>68.61</b>	<b>55.53</b>	<b>16.95</b>	<b>80.22</b>	<b>78.03</b>	72.95	58.62	13.77	<b>71.64</b>	<b>67.99</b>	<b>61.79</b>	49.72	21.43
+VL-NMS R	76.46	73.62	68.56	55.46	16.85	79.87	77.92	<b>73.27</b>	58.02	13.65	70.32	66.89	61.43	<b>50.97</b>	<b>21.81</b>
CM-A-E [3]†	76.75	73.98	69.06	55.65	16.93	81.23	79.28	74.30	<b>60.19</b>	<b>14.21</b>	70.09	66.38	60.92	49.66	21.33
+VL-NMS B	<b>78.91</b>	<b>75.70</b>	<b>70.31</b>	56.56	<b>17.34</b>	<b>82.11</b>	<b>80.01</b>	74.95	60.12	14.05	<b>73.66</b>	<b>70.05</b>	<b>63.69</b>	51.17	21.88
+VL-NMS R	78.05	75.09	70.05	<b>56.77</b>	17.27	81.72	79.64	<b>75.09</b>	59.48	14.04	71.93	68.38	62.77	<b>52.01</b>	<b>22.30</b>

TABLE X  
RES PERFORMANCE (%) OF DIFFERENT ARCHITECTURES WITH PR@X METRIC ON REFCOCO+. † DENOTES THAT THE RESULTS ARE FROM OUR REIMPLEMENTATION USING OFFICIAL RELEASED CODES.

Models	val					testA					testB				
	0.5	0.6	0.7	0.8	0.9	0.5	0.6	0.7	0.8	0.9	0.5	0.6	0.7	0.8	0.9
MAttNet [1]†	64.71	62.44	58.54	47.76	14.33	<b>70.12</b>	<b>68.44</b>	63.87	<b>51.89</b>	<b>12.29</b>	56.00	52.85	48.27	39.23	17.24
+VL-NMS B	<b>65.16</b>	<b>62.82</b>	<b>58.74</b>	47.69	14.37	69.61	67.78	63.41	50.38	12.03	<b>57.13</b>	<b>53.63</b>	48.89	39.17	16.55
+VL-NMS R	65.01	62.60	58.66	<b>47.79</b>	<b>14.50</b>	69.91	68.25	<b>64.11</b>	51.24	11.95	56.35	53.41	<b>49.15</b>	<b>39.97</b>	<b>17.39</b>
NMTTree [2]†	65.24	62.92	58.98	47.56	14.34	69.89	68.11	63.64	<b>52.03</b>	12.38	56.49	53.32	49.21	39.33	17.30
+VL-NMS B	65.44	62.96	58.81	47.33	14.52	69.93	67.88	63.43	50.87	<b>12.45</b>	57.03	53.65	49.09	39.19	16.49
+VL-NMS R	<b>65.54</b>	<b>63.15</b>	<b>59.07</b>	<b>47.59</b>	<b>14.58</b>	<b>70.21</b>	<b>68.46</b>	<b>64.02</b>	51.50	11.91	<b>57.21</b>	<b>54.45</b>	<b>50.19</b>	<b>40.54</b>	<b>17.43</b>
CM-A-E [3]†	66.98	<b>64.60</b>	<b>60.63</b>	<b>49.15</b>	14.73	71.46	69.70	65.14	<b>53.23</b>	12.31	57.13	53.92	49.34	40.17	<b>17.55</b>
+VL-NMS B	66.48	63.93	59.98	48.39	14.81	<b>71.80</b>	69.82	65.18	52.41	<b>12.64</b>	<b>57.74</b>	<b>54.71</b>	<b>49.66</b>	40.21	16.90
+VL-NMS R	<b>67.01</b>	64.58	60.62	48.99	<b>14.88</b>	71.73	<b>69.89</b>	<b>65.46</b>	52.62	12.10	56.80	53.96	49.40	<b>40.36</b>	17.26

- [11] J. Mao, J. Huang, A. Toshev, O. Camburu, A. L. Yuille, and K. Murphy, "Generation and comprehension of unambiguous object descriptions," in *CVPR*, 2016.
- [12] T.-Y. Lin, M. Maire, S. Belongie, J. Hays, P. Perona, D. Ramanan, P. Dollár, and C. L. Zitnick, "Microsoft coco: Common objects in context," in *ECCV*, 2014.
- [13] P. Anderson, X. He, C. Buehler, D. Teney, M. Johnson, S. Gould, and L. Zhang, "Bottom-up and top-down attention for image captioning and visual question answering," in *CVPR*, 2018.
- [14] A. R. Akula, S. Gella, Y. Al-Onaizan, S.-C. Zhu, and S. Reddy, "Words aren't enough, their order matters: On the robustness of grounding visual referring expressions," in *ACL*, 2020.
- [15] L. Chen, W. Ma, J. Xiao, H. Zhang, and S.-F. Chang, "Ref-nms: Breaking proposal bottlenecks in two-stage referring expression grounding," in *AAAI*, 2021.
- [16] R. Hu, M. Rohrbach, J. Andreas, T. Darrell, and K. Saenko, "Modeling relationships in referential expressions with compositional modular networks," in *CVPR*, 2017.
- [17] R. Hu, H. Xu, M. Rohrbach, J. Feng, K. Saenko, and T. Darrell, "Natural language object retrieval," in *CVPR*, 2016.
- [18] L. Yu, P. Poirson, S. Yang, A. C. Berg, and T. L. Berg, "Modeling context in referring expressions," in *ECCV*, 2016.
- [19] L. Yu, H. Tan, M. Bansal, and T. L. Berg, "A joint speaker-listener-reinforcer model for referring expressions," in *CVPR*, 2017.
- [20] R. Hu, M. Rohrbach, and T. Darrell, "Segmentation from natural language expressions," in *ECCV*, 2016.
- [21] C. Liu, Z. Lin, X. Shen, J. Yang, X. Lu, and A. Yuille, "Recurrent multimodal interaction for referring image segmentation," in *ICCV*, 2017.
- [22] H. Shi, H. Li, F. Meng, and Q. Wu, "Key-word-aware network for referring expression image segmentation," in *ECCV*, 2018.
- [23] E. Margffoy-Tuay, J. C. Pérez, E. Botero, and P. Arbeláez, "Dynamic multimodal instance segmentation guided by natural language queries," in *ECCV*, 2018.
- [24] D. Liu, H. Zhang, Z.-J. Zha, M. Wang, and Q. Sun, "Joint visual grounding with language scene graphs," in *arXiv*, 2019.
- [25] R. Hong, D. Liu, X. Mo, X. He, and H. Zhang, "Learning to compose and reason with language tree structures for visual grounding," *TPAMI*, 2019.
- [26] Y. Niu, H. Zhang, Z. Lu, and S.-F. Chang, "Variational context: Exploiting visual and textual context for grounding referring expressions," *TPAMI*, 2019.
- [27] P. Wang, Q. Wu, J. Cao, C. Shen, L. Gao, and A. v. d. Hengel, "Neighbourhood watch: Referring expression comprehension via language-guided graph attention networks," in *CVPR*, 2019.
- [28] S. Yang, G. Li, and Y. Yu, "Graph-structured referring expression reasoning in the wild," in *CVPR*, 2020.
- [29] X. Chen, L. Ma, J. Chen, Z. Jie, W. Liu, and J. Luo, "Real-time referring expression comprehension by single-stage grounding network," in *arXiv*, 2018.
- [30] Z. Yang, B. Gong, L. Wang, W. Huang, D. Yu, and J. Luo, "A fast and accurate one-stage approach to visual grounding," in *ICCV*, 2019.
- [31] Y. Liao, S. Liu, G. Li, F. Wang, Y. Chen, C. Qian, and B. Li, "A real-time cross-modality correlation filtering method for referring expression comprehension," in *CVPR*, 2020.
- [32] G. Luo, Y. Zhou, X. Sun, L. Cao, C. Wu, C. Deng, and R. Ji, "Multi-task collaborative network for joint referring expression



TABLE XI  
RES PERFORMANCE (%) OF DIFFERENT ARCHITECTURES WITH PR@X METRIC ON RefCOCO. † DENOTES THAT THE RESULTS ARE FROM OUR REIMPLEMENTATION USING OFFICIAL RELEASED CODES.

Models	val					test				
	0.5	0.6	0.7	0.8	0.9	0.5	0.6	0.7	0.8	0.9
MAttNet [1]†	65.28	62.25	56.96	44.36	14.67	65.93	63.14	57.51	44.62	12.61
+VL-NMS B	66.03	62.70	57.09	44.34	14.73	<b>66.58</b>	<b>63.49</b>	<b>57.82</b>	45.21	13.03
+VL-NMS R	<b>66.26</b>	<b>63.38</b>	<b>57.74</b>	<b>44.93</b>	<b>15.09</b>	65.86	62.83	57.24	<b>45.26</b>	<b>13.12</b>
NMTTree [2]†	63.32	60.21	55.23	42.99	14.56	64.43	61.58	56.31	43.88	12.57
+VL-NMS B	<b>64.40</b>	61.01	55.54	43.10	14.69	<b>64.94</b>	<b>61.87</b>	<b>56.34</b>	44.28	12.98
+VL-NMS R	64.01	<b>61.07</b>	<b>55.86</b>	<b>43.67</b>	<b>15.20</b>	64.54	61.41	56.09	<b>44.62</b>	<b>13.25</b>
CM-A-E [3]†	66.32	63.01	57.86	44.71	14.85	67.63	64.62	59.12	45.77	13.21
+VL-NMS B	<b>67.75</b>	<b>64.11</b>	<b>58.35</b>	<b>45.40</b>	15.16	<b>68.49</b>	<b>65.28</b>	<b>59.51</b>	46.50	13.52
+VL-NMS R	66.52	63.52	58.03	45.04	<b>15.28</b>	68.29	65.06	59.48	<b>46.96</b>	<b>13.82</b>

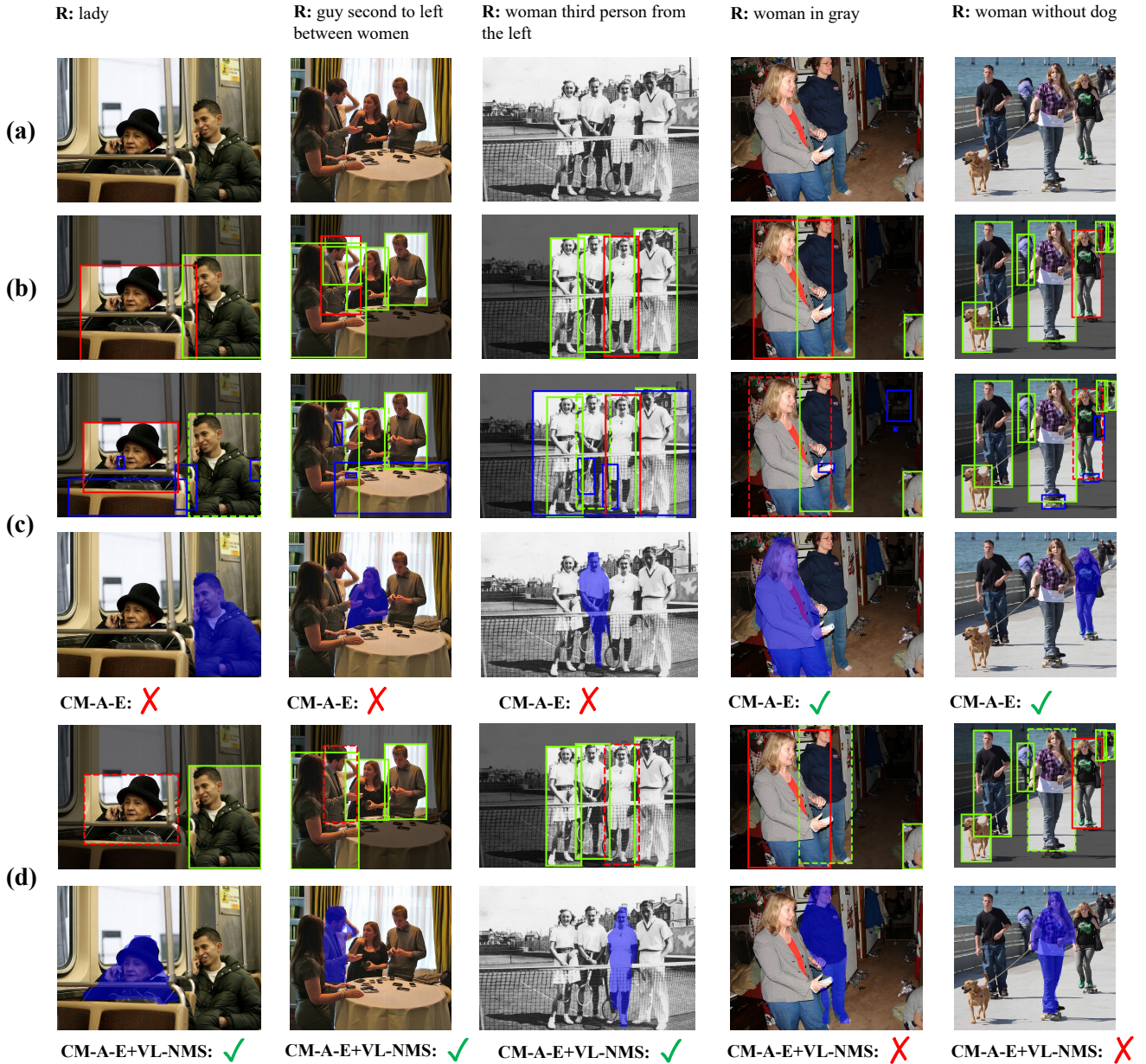


Fig. 7. Qualitative REC and RES results on RefCOCO, arranged in a similar style to Figure 6.



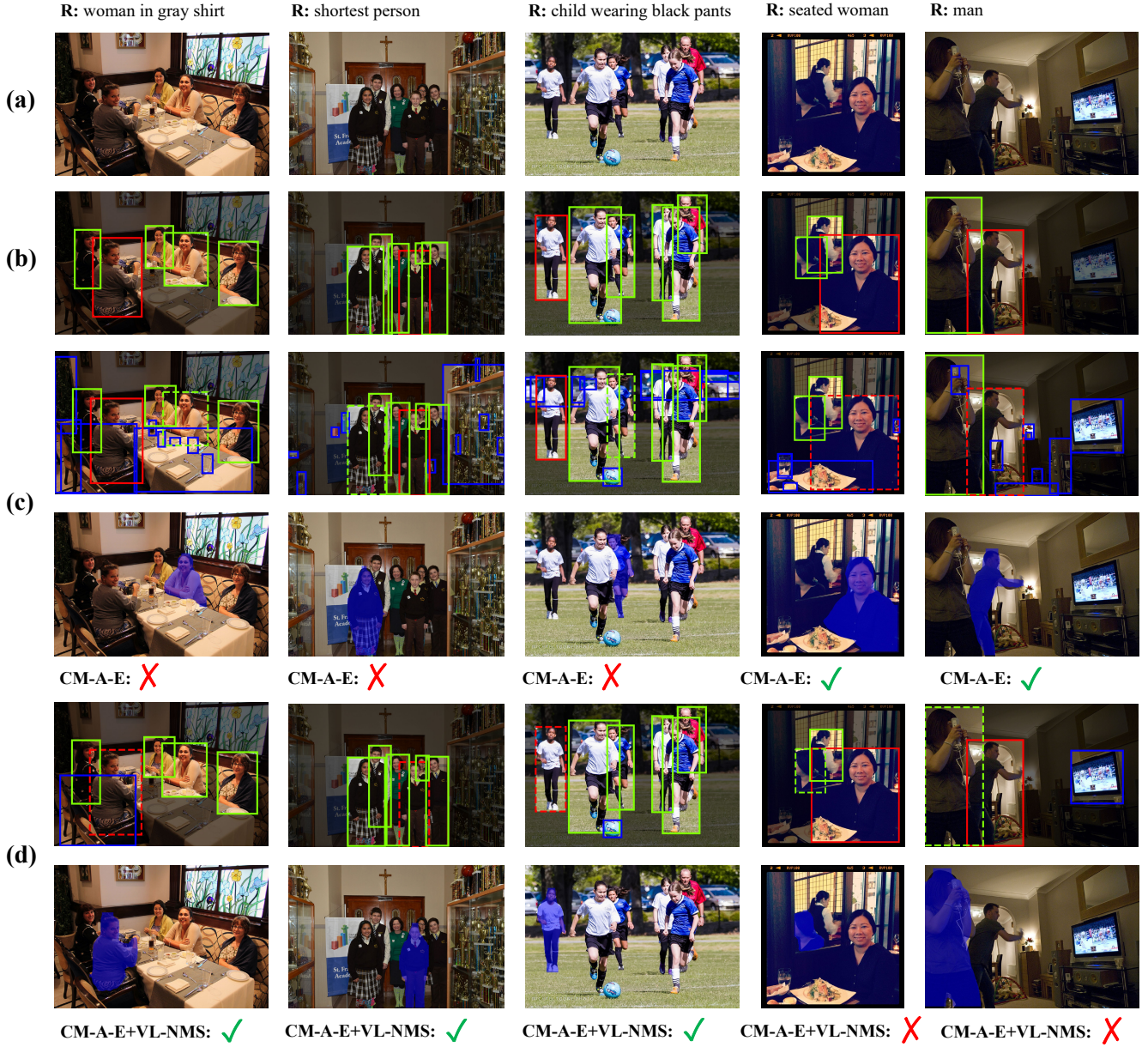


Fig. 8. Qualitative REC and RES results on RefCOCO+, arranged in a similar style to Figure 6.

- comprehension and segmentation,” in *CVPR*, 2020.
- [33] Z. Yang, T. Chen, L. Wang, and J. Luo, “Improving one-stage visual grounding by recursive sub-query construction,” in *ECCV*, 2020.
- [34] R. Li, K. Li, Y.-C. Kuo, M. Shu, X. Qi, X. Shen, and J. Jia, “Referring image segmentation via recurrent refinement networks,” in *CVPR*, 2018.
- [35] D.-J. Chen, S. Jia, Y.-C. Lo, H.-T. Chen, and T.-L. Liu, “See-through-text grouping for referring image segmentation,” in *ICCV*, 2019.
- [36] S. Huang, T. Hui, S. Liu, G. Li, Y. Wei, J. Han, L. Liu, and B. Li, “Referring image segmentation via cross-modal progressive comprehension,” in *CVPR*, 2020.
- [37] L. Ye, M. Rochan, Z. Liu, and Y. Wang, “Cross-modal self-attention network for referring image segmentation,” in *CVPR*, 2019.
- [38] Z. Hu, G. Feng, J. Sun, L. Zhang, and H. Lu, “Bi-directional relationship inferring network for referring image segmentation,” in *CVPR*, 2020.
- [39] K. He, G. Gkioxari, P. Dollár, and R. Girshick, “Mask r-cnn,” in *ICCV*, 2017.
- [40] L. Wang, Y. Li, and S. Lazebnik, “Learning deep structure-preserving image-text embeddings,” in *CVPR*, 2016.
- [41] F. Faghri, D. J. Fleet, J. R. Kiros, and S. Fidler, “Vse++: Improving visual-semantic embeddings with hard negatives,” in *arXiv*, 2017.
- [42] Y. Wu, S. Wang, and Q. Huang, “Learning semantic structure-preserved embeddings for cross-modal retrieval,” in *ACM MM*, 2018.
- [43] Z. Yu, J. Yu, C. Xiang, Z. Zhao, Q. Tian, and D. Tao, “Rethinking diversified and discriminative proposal generation for visual grounding,” in *IJCAI*, 2018.
- [44] K. Chen, R. Kovvuri, and R. Nevatia, “Query-guided regression network with context policy for phrase grounding,” in *ICCV*, 2017.
- [45] K. Chen, J. Gao, and R. Nevatia, “Knowledge aided consistency

- for weakly supervised phrase grounding,” in *CVPR*, 2018.
- [46] S. Datta, K. Sikka, A. Roy, K. Ahuja, D. Parikh, and A. Diwakaran, “Align2ground: Weakly supervised phrase grounding guided by image-caption alignment,” in *ICCV*, 2019.
  - [47] T. Gupta, A. Vahdat, G. Chechik, X. Yang, J. Kautz, and D. Hoiem, “Contrastive learning for weakly supervised phrase grounding,” in *ECCV*, 2020.
  - [48] B. Jiang, R. Luo, J. Mao, T. Xiao, and Y. Jiang, “Acquisition of localization confidence for accurate object detection,” in *ECCV*, 2018.
  - [49] L. Tychsen-Smith and L. Petersson, “Improving object localization with fitness nms and bounded iou loss,” in *CVPR*, 2018.
  - [50] Z. Tan, X. Nie, Q. Qian, N. Li, and H. Li, “Learning to rank proposals for object detection,” in *ICCV*, 2019.
  - [51] C. Yang, V. Ablavsky, K. Wang, Q. Feng, and M. Betke, “Learning to separate: Detecting heavily-occluded objects in urban scenes,” in *arXiv*, 2019.
  - [52] J. Hosang, R. Benenson, and B. Schiele, “Learning non-maximum suppression,” in *CVPR*, 2017.
  - [53] H. Hu, J. Gu, Z. Zhang, J. Dai, and Y. Wei, “Relation networks for object detection,” in *CVPR*, 2018.
  - [54] N. Bodla, B. Singh, R. Chellappa, and L. S. Davis, “Soft-nms—improving object detection with one line of code,” in *ICCV*, 2017.
  - [55] S. Liu, D. Huang, and Y. Wang, “Adaptive nms: Refining pedestrian detection in a crowd,” in *CVPR*, 2019.
  - [56] S. Yang, G. Li, and Y. Yu, “Dynamic graph attention for referring expression comprehension,” in *ICCV*, 2019.
  - [57] L. Chen, H. Zhang, J. Xiao, L. Nie, J. Shao, W. Liu, and T.-S. Chua, “Sca-cnn: Spatial and channel-wise attention in convolutional networks for image captioning,” in *CVPR*, 2017.
  - [58] S. Kazemzadeh, V. Ordonez, M. Matten, and T. Berg, “Referitgame: Referring to objects in photographs of natural scenes,” in *EMNLP*, 2014.
  - [59] V. K. Nagaraja, V. I. Morariu, and L. S. Davis, “Modeling context between objects for referring expression understanding,” in *ECCV*, 2016.
  - [60] H. Zhang, Y. Niu, and S.-F. Chang, “Grounding referring expressions in images by variational context,” in *CVPR*, 2018.
  - [61] B. Zhuang, Q. Wu, C. Shen, I. Reid, and A. van den Hengel, “Parallel attention: A unified framework for visual object discovery through dialogs and queries,” in *CVPR*, 2018.
  - [62] P. Young, A. Lai, M. Hodosh, and J. Hockenmaier, “From image descriptions to visual denotations: New similarity metrics for semantic inference over event descriptions,” *TACL*, 2014.
  - [63] S. Xiao, L. Chen, S. Zhang, W. Ji, J. Shao, L. Ye, and J. Xiao, “Boundary proposal network for two-stage natural language video localization,” in *AAAI*, 2021.
  - [64] L. Chen, C. Lu, S. Tang, J. Xiao, D. Zhang, C. Tan, and X. Li, “Rethinking the bottom-up framework for query-based video localization,” in *AAAI*, 2020.
  - [65] L. Chen, X. Yan, J. Xiao, H. Zhang, S. Pu, and Y. Zhuang, “Counterfactual samples synthesizing for robust visual question answering,” in *CVPR*, 2020.